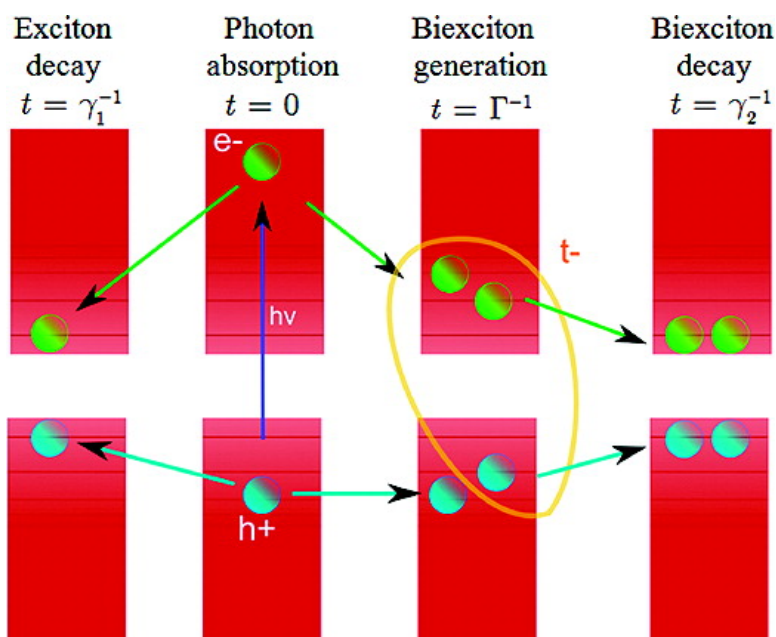


Distribution of Multiexciton Generation Rates in CdSe and InAs Nanocrystals

Ernan Rabani, and Roi Baer

Nano Lett., **2008**, 8 (12), 4488-4492 • Publication Date (Web): 29 October 2008

Downloaded from <http://pubs.acs.org> on December 20, 2008



More About This Article

Additional resources and features associated with this article are available within the HTML version:

- Supporting Information
- Access to high resolution figures
- Links to articles and content related to this article
- Copyright permission to reproduce figures and/or text from this article

[View the Full Text HTML](#)

Distribution of Multiexciton Generation Rates in CdSe and InAs Nanocrystals

Eran Rabani*[†] and Roi Baer*[‡]

School of Chemistry, The Raymond and Beverly Sackler Faculty of Exact Sciences, Tel Aviv University, Tel Aviv 69978 Israel, and Institute of Chemistry and the Fritz Haber Center for Molecular Dynamics, The Hebrew University of Jerusalem, Jerusalem 91904 Israel

Received August 11, 2008; Revised Manuscript Received October 6, 2008

ABSTRACT

The distribution of rates of multiexciton generation following photon absorption is calculated for semiconductor nanocrystals (NCs). The rates of biexciton generation are calculated using Fermi's golden rule with all relevant Coulomb matrix elements, taking into account proper selection rules within a screened semiempirical pseudopotential approach. In CdSe and InAs NCs, we find a broad distribution of biexciton generation rates depending strongly on the exciton energy and size of the NC. Multiexciton generation becomes inefficient for NCs exceeding 3 nm in diameter in the photon energy range of 2–3 times the band gap.

Multiexciton generation (MEG) is a process where several excitons are generated upon the absorption of a single photon in semiconductors.¹ MEG is of potential significance for improving the efficiency of light harvesting devices, such as solar cells.² Strict selection rules and competing processes in the bulk allow generation of multiexcitons at energies of $n \times E_g$ where E_g is the band gap and $n > 3$; however, truly efficient MEG is observed only for $n > 5$.³ It was suggested² that nanocrystals (NCs), where quantum confinement effects are important, may exhibit MEG at lower values of n (typically 2–3).² Indeed, MEG in NCs has been reported recently for several systems,^{4–8} showing that the threshold was size and band gap independent.^{5,6,8} However, more recent studies have questioned the efficiency of MEG in NCs, in particular for CdSe⁹ and InAs.¹⁰ The goal of the present Letter is to address this controversy.

The theory of MEG in bulk is based on the concept of impact ionization.¹¹ The absorbed photon creates two charge carriers: a negative electron and a positive hole, each having an effective mass depending on the band structure of the crystal. The lighter particle of the pair takes most of the kinetic energy and eventually loses part of this energy by creating additional charge carriers (see Figure 1). For NCs, a similar mechanism exists and several theoretical approaches, some based on a coherent MEG^{5,7,12} and others on an incoherent MEG^{13,14} have been proposed. A condition for efficient MEG common to all approaches is that the rate of exciton decay be smaller than the rate of multiexciton generation $\gamma_1 < \Gamma$ (see Figure 1). In solids, the principal

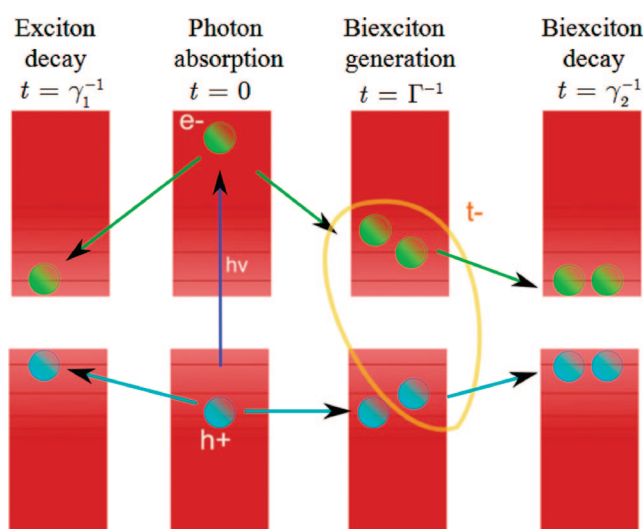


Figure 1. Impact ionization mechanism for biexciton generation in NCs. After absorption of a photon at time $t = 0$ an exciton (electron–hole pair) is formed. This exciton can either decay to the band edge within time scale of $\gamma_1^{-1} \approx 1$ ps¹⁵ or within Γ^{-1} to a biexcitonic state. A biexciton decays to the band-edge at rate $\gamma_2 \approx 2$ ps⁻¹.¹³ In this example, the excited electron e^- (hole h^+) decays to a negative (positive) three-particle entity called a trion t^- (t^+).

mechanism for exciton decay is the phonon-assisted carrier relaxation, with lifetimes of the order of subpicoseconds to picosecond.¹⁵ Somewhat unexpectedly, experimental investigations of exciton decay in CdSe and PbSe NCs indicate that the rate of near-band edge exciton decay is of the same order of magnitude as seen in bulk and even grows as the dot size decreases.¹⁶ At photon energies well above twice the gap, the threshold energy for biexciton generation, the density

[†] Tel Aviv University.

[‡] The Hebrew University of Jerusalem.

of hole and electron states is usually high and it is reasonable to expect that near-bulk relaxation rates apply as well.

Despite the initial existing theoretical and experimental work, there is not yet available a detailed reliable theoretical estimate of MEG rates. Such a feat requires: (a) A quantitative accurate account of the electronic structure of the NC, especially the highly excited states. (b) A description of the dense manifold of single and multiexcitonic states. (c) A theory of electron correlation that can explain the formation of multiexcitons fully consistent with the single particle electronic structure. So far, theoretical treatments of MEG in NCs have not met all three requirements at once: the work in ref 14 is based on a tight-binding model which may not be accurate enough at high excitation energies and the ab initio calculation¹⁷ of MEG rates in small clusters is not of obvious relevance for NCs.

In this Letter, we present a framework that meets the above requirements. Using an atomistic semiempirical pseudopotential method that captures realistically the density of electronic states, we deduce the density of excitons and biexcitons and calculate the Coulomb matrix elements even at energies high above the band gap. The detailed framework we develop allows us to study the effect of NC size (up to a diameter of ~ 3 nm and ~ 2000 electrons), photon energy (up to $3E_g$), and composition (CdSe and InAs NCs) on the process of MEG.

We consider MEG for two prototype NCs, CdSe (II–VI) and InAs (III–V). The local screened pseudopotentials were fitted to reproduce the experimental bulk band gap and effective masses for CdSe¹⁸ and InAs,¹⁹ neglecting spin–orbit coupling.²⁰ Furthermore, ligand potentials are used to represent the passivation layer.¹⁸ The resulting single-particle Schrödinger equation is solved in real space by the filter-diagonalization (FD) technique.²¹ FD allows construction of an eigensubspace of all energy levels up to $3E_g$ above the Fermi energy. From this, the density of states (DOS) is calculated by energy binning. As a check on the FD we also employed an alternative Monte Carlo method²² which computes directly the DOS

$$\pi^{-1} \text{ImTr}[(e - H + i\gamma)^{-1}]$$

(for the results shown, $\gamma = 0.1$ eV). Using binning or self-convolutions of the DOS, the exciton (DOSX) and biexciton (DOSXX) density of states can be determined.

The calculated DOSX and DOSXX are shown in Figure 2 for CdSe and InAs NCs for various sizes. The excitonic threshold occurs by definition at $E = E_g$. The two methods of calculating the DOSX agree well, indicating that the FD method is well converged, and all states are generated within the energy window up to $3E_g$. The biexcitonic threshold is $2E_g$. For higher energies the DOSXX grows with energy at a considerably faster rate than the DOSX, overtaking it at scaled energies which only slightly depend on the size and composition of the NCS (between 2.3 and $2.5E_g$). The onset of MEG in PbSe at around $2.2E_g$ has been attributed to this crossing.¹³ However, it still remains an open question whether this crossing is indeed relevant for efficient MEG. As we argue below, DOSXX is *not* the relevant density of states to

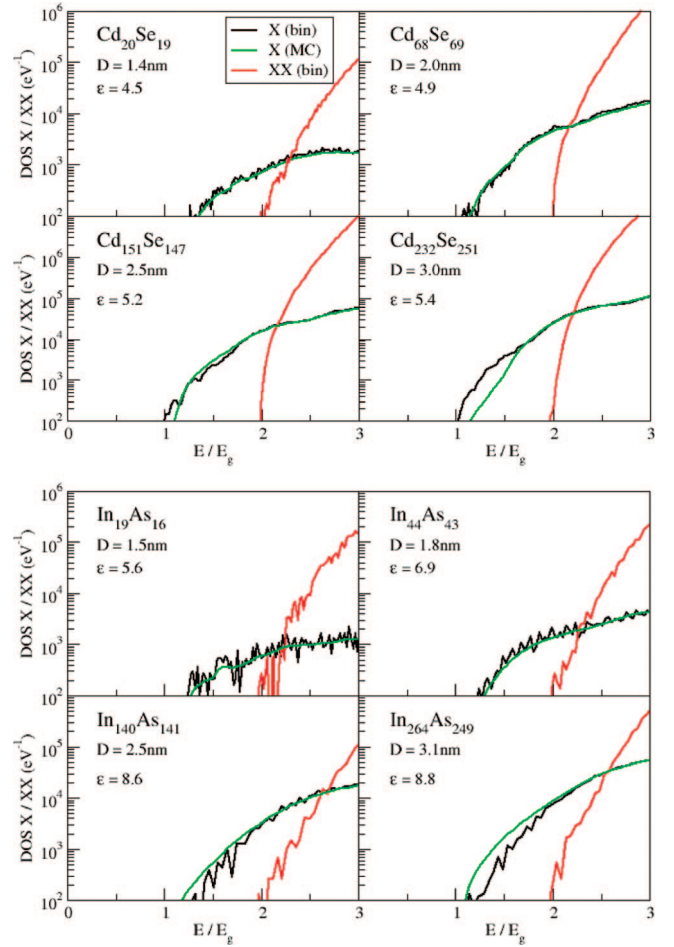


Figure 2. The density of single excitons (DOSX) and biexcitons (DOSXX) in various CdSe (upper panels) and InAs (lower panels) NCs.

consider because of the strict selection rules dictated by the exciton–biexciton coupling elements.

The process of MEG involves the conversion of an exciton, of say spin up,

$$|S_{it}^{\uparrow}\rangle = a_{it}^{\dagger} a_{it} |0\rangle$$

to a biexciton

$$|B_{jokst}^{cabot}\rangle = a_{bot}^{\dagger} a_{co}^{\dagger} a_{jo} a_{kst} |0\rangle$$

which is a state of two coexisting excitons. Here $|0\rangle$ is the ground-state determinant wave function where all hole states are occupied by electrons; $a_{i\sigma}$ ($a_{i\sigma}^{\dagger}$) are electron annihilation (creation) operators into the molecular orbital $\psi_i(\mathbf{r})$ with spin σ (obtained from the pseudopotential calculation). In the following, we use the index convention that $i, j,$ and k designate hole orbitals; and $a, b,$ and c electron orbitals while r, s, t and u are general orbital indices. The rate of decay of a single exciton into biexcitons is given by Fermi's golden rule:

$$\Gamma_{iat} = \frac{2\pi}{\hbar} \sum_{jkbct\sigma'} |W_{ia}^{bjkj,\sigma\sigma'}|^2 \delta[(\epsilon_a - \epsilon_i) - (\epsilon_b - \epsilon_k + \epsilon_c - \epsilon_j)] \quad (1)$$

where

$$W_{ia}^{bkcj,\sigma\sigma'} = \left\langle S_{it}^{\sigma\dagger} \left| \sum_{rsut\sigma''\sigma'''} \frac{1}{2} V_{rsut} a_{rs}^{\dagger} a_{rt}^{\dagger} a_{u\sigma''}^{\dagger} a_{t\sigma'''}^{\dagger} a_{sa} B_{jokot}^{b\sigma\sigma'} \right. \right\rangle \quad (2)$$

and

$$V_{rsut} = \iint d^3r d^3r' [\psi_r(\mathbf{r})\psi_s(\mathbf{r})\psi_u(\mathbf{r}')\psi_t(\mathbf{r}')/\epsilon|\mathbf{r}-\mathbf{r}'|] \quad (3)$$

Here ϵ is the dielectric constant of the NC, estimated from ref 23 for CdSe and ref 19 for InAs. Deploying Fermionic commutation rules and energy conservation requirements, it is possible to develop the matrix element in eq 2 and show that the decay of exciton $S_{ia,\uparrow}$ to biexciton involves *either* the decay of the electron at ψ_a or the decay of the hole at ψ_i but not both: one of the two particles is active while the other is a spectator. The simultaneous involvement of both particles in the process is a higher order perturbation term and is neglected in the present treatment. The process we consider therefore involves a decay of the electron (hole) in state ψ_a (ψ_i) of energy ϵ_a (ϵ_i) to a negative (positive) three particle charged state called a trion. The trion is composed of two electrons (holes), respectively, in states ψ_b and ψ_c (ψ_j and ψ_k) and a hole (electron) in state ψ_i (ψ_a). The trion must have the same energy as the parent electron (hole) so $\epsilon_a = \epsilon_b + \epsilon_c - \epsilon_j$ ($\epsilon_i = \epsilon_k + \epsilon_j - \epsilon_b$). The total decay rate can be written as the sum of rates $\Gamma_{ia} = \Gamma_{ia}^+ + \Gamma_{ia}^-$, given by Fermi's golden rule:

$$\Gamma_i^+ = \frac{4\pi}{\hbar} \sum_{jkb} |(2V_{jikb} - V_{kijb})|^2 \delta(\epsilon_i - (\epsilon_k + \epsilon_j - \epsilon_b))$$

$$\Gamma_a^- = \frac{4\pi}{\hbar} \sum_{cbj} |(2V_{acjb} - V_{abjc})|^2 \delta(\epsilon_a - (\epsilon_b + \epsilon_c - \epsilon_j)) \quad (4)$$

In Figure 3, we show calculation results based on this theory for CdSe (left panels) and InAs (right panels) at two sizes

of NCs for exciton energies in the $2-3E_g$ range. Each point in the figure represents an exciton $|S_{is}\rangle$ of a scaled energy $(\epsilon_a - \epsilon_i)/E_g$. The lowest panel depicts the density of trion states (DOTS): positive trions are black points with DOTS

$$\rho_{ia}^+ = \sum_{jkb} \delta(\epsilon_i + \epsilon_b - \epsilon_k - \epsilon_j)$$

and negative trions are red points with DOTS

$$\rho_{ia}^- = \sum_{cbj} \delta(\epsilon_a + \epsilon_j - \epsilon_b - \epsilon_c)$$

All results shown were obtained using a window representing the δ function of width 0.06 eV (results were not sensitive to widths above this value). It is seen that the number of black points is much smaller than the number of red points. Similar to the situation in the bulk, the low mass particle takes most of the exciton energy, which for both CdSe and InAs is the electron. Thus there are many more negative trions in resonance with the electron than positive trions in resonance with the hole. In the bulk the lighter particle takes most of the kinetic energy because both must have equal momentum. In NCs with strong confinement, this same result is due to the fact that the DOS near the band edge grows with the particle mass, so heavier (lighter) particles have a large (small) density of states near the band edge.

The upper panels in Figure 3 show the decay rate for each exciton (see eq 4): Γ_{ia}^+ via a positive trion or Γ_{ia}^- via a negative trion. An effective Coulomb matrix element, defined as

$$W_{ia}^{\pm} = \sqrt{\hbar\Gamma_{ia}^{\pm}/(2\pi\rho_{ia}^{\pm})}$$

is shown in the center panels.

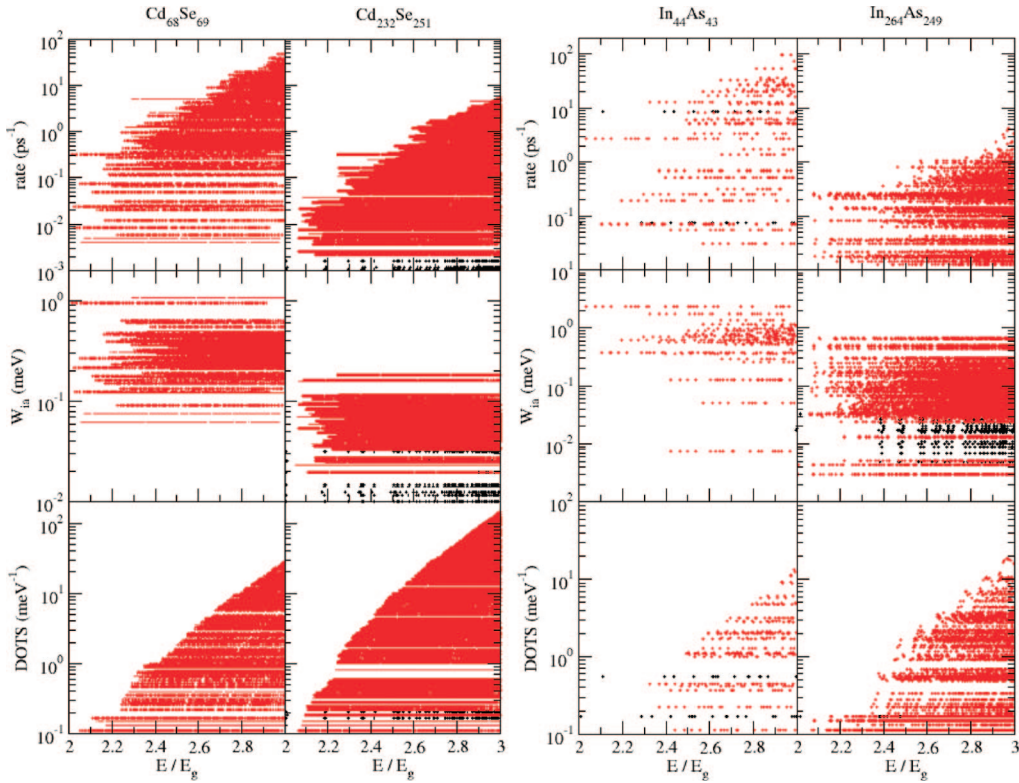


Figure 3. The rate of exciton–biexciton transition given by eq 4 (upper panels), Coulomb coupling W_{ia}^{\pm} (middle panels), and DOTS ρ_{ia}^{\pm} (lower panels) in the energy range of $2-3E_g$ for two NCs of CdSe (left panels) and InAs (right panels). Black (red) points represent excitons decaying to electron (hole) + positive (negative) trions.

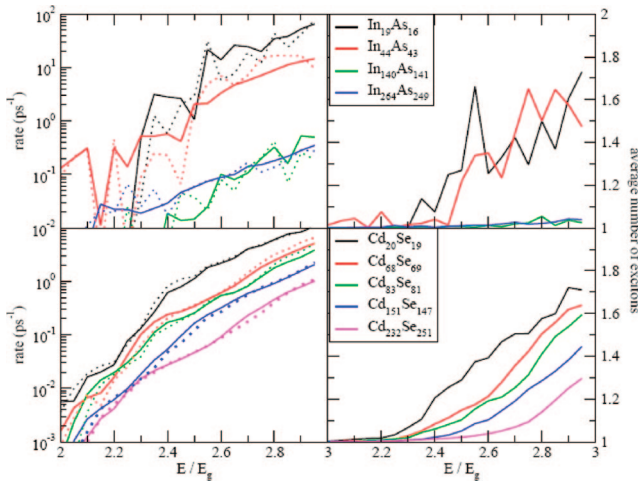


Figure 4. Left: the average rate of exciton to biexciton transition in various InAs (upper) and CdSe (lower) NCs vs the photon energy. Right: the average number of excitons generated in various InAs (upper) and CdSe (lower) NCs.

There are several important conclusions drawn from the results shown in Figure 3:

(a) In CdSe the DOTS increases at a given scaled energy as the size of the NC grows. In InAs this behavior is much weaker. At a given energy the DOTS of a NC increases with size, however, at a *scaled* energy, since E_g decreases with size, such size dependence is weaker. In InAs the strong confinement makes E_g highly sensitive to size causing a reduced sensitivity of the DOTS as a function of the scaled energy. Overall there are fewer trion states for InAs compared to CdSe because E_g is smaller in the former NC; thus the absolute energy probed and the corresponding DOTS are lower.

(b) The effective coupling W_{ia}^{\pm} for a given exciton is nearly energy independent, approximately equals to 0.1–1 meV depending on the size of the NC, with a spread that decreases with NC size and spans 1–2 orders of magnitude. NCs of smaller diameter D exhibit larger coupling elements. However, the coupling is not proportional to D^{-1} as expected when the states scale linearly with D (for example, for a particle in a sphere).

(c) The rate of exciton–biexciton transition at a given exciton energy spans 4–6 orders of magnitude, depending on the specific exciton (i and a). Thus, conclusions regarding the MEG process require the calculation of the rate for *all* excitons in a given energy and may not be drawn from a limited arbitrary set of excitons. We find that due to quantum confinement, the smaller NCs span a larger range of rates. In addition, smaller NCs have smaller DOTS but larger W_{ia}^{\pm} . The net effect of combining the two quantities into the rate results in a larger rate for smaller NCs at a given scaled energy.

In Figure 4 (left panels) we show the average rate of exciton to biexciton transition for various InAs and CdSe NCs. Two averaging schemes are used yielding similar results. One is a straightforward arithmetic average (solid lines) and the other is an oscillator strength weighted average (dotted line). As discussed above, the transition rate decreases

with NC size D at a given *scaled* energy E/E_g . However, since the band gap decreases with increasing NC size, a similar plot at a given *absolute* energy yields an *opposite* effect.

There are two main factors that influence the dependence of MEG rate on the size of the NC, the DOTS and the effective coupling W_{ia}^{\pm} . The DOTS increases with energy and mildly with D while the effective coupling decreases strongly with D (due to the decreasing Coulomb matrix element and the increasing dielectric constant) and is nearly exciton-energy independent. The MEG rate, which is proportional to the product of the two, inherits its dependence on the energy from the DOTS while its dependence on D from W_{ia}^{\pm} .

The number of final excitons produced by a photon can be estimated using a kinetic model and is given by

$$N_{\text{ex}}(E) = \sum_{ia} p_{ia}(E)(2\Gamma_{ia} + \gamma)/(\Gamma_{ia} + \gamma)$$

where $p_{ia}(E)$ is the probability of generating the exciton S_{ia} and $\gamma = 3 \text{ ps}^{-1}$ is the decay rate of a single exciton to its lowest state.²⁴ We plot $N_{\text{ex}}(E)$ for InAs and CdSe NCs in Figure 4 (right panels). MEG should be observed when $\Gamma_{ia} > \gamma$ as is the case for the smallest NCs. For larger NCs the efficiency of MEG decreases significantly in InAs and somewhat less so in CdSe. This is consistent with known results for bulk and is in agreement with recent experimental results on CdSe⁹ and InAs¹⁰ for NCs of $D \geq 5 \text{ nm}$. The measurement on CdSe NCs with $D = 3.2 \text{ nm}$ ⁷ is a border case, and we predict that MEG may occur for this system depending on the value of γ . Our results disagree with one experiment, namely, the positive MEG in InAs⁸ at $D = 4.3 \text{ nm}$. We argue that the onset of MEG should be observable only for energies larger than $3E_g$ but not at $2E_g$ where our prediction for the exciton–biexciton transition rate is approximately 0.01 ps^{-1} . Other materials require explicit calculation of the MEG rate; however, we anticipate that a similar picture will emerge.

In summary, we have carried out detailed calculations of the exciton–biexciton transition rate using Fermi’s golden rule for CdSe and InAs NCs at different sizes and in the energy range of $2\text{--}3E_g$. We use the highly reliable semiempirical atomistic electronic structure method and introduce Coulomb coupling between excitons and biexcitons in a consistent way via a perturbation theory. We do not find evidence that the MEG is correlated with the crossover of DOSX and DOSXX, since the relevant density of states entering Fermi’s golden rule is the DOTS. We predict that there is a wide spread of rates (several orders of magnitude) for different excitons at a given energy dominated by decay to negative trions. The average rate is strongly size and energy dependent. For CdSe and InAs NCs with diameter larger than 3 nm , we argue that MEG below $3E_g$ is of low efficiency, but at higher energies or smaller NCs, MEG can become efficient.

Acknowledgment. This research was supported by the Converging Technologies Program of The Israel Science Foundation (Grant Number 1704/07) and The Israel Science Foundation (Grant Number 962/06).

References

- (1) Vavilov, V. S. *Sov. Phys. Usp.* **1962**, *4*, 761.
- (2) Nozik, A. J. *Physica E* **2002**, *14*, 115.
- (3) Kolodinski, S.; Werner, J. H.; Wittchen, T.; Queisser, H. J. *Appl. Phys. Lett.* **1993**, *63*, 2405. Christensen, O. *J. Appl. Phys.* **1976**, *47*, 689.
- (4) Schaller, R. D.; Klimov, V. I. *Phys. Rev. Lett.* **2004**, *92*, 186601. Klimov, V. I. *J. Phys. Chem. B* **2006**, *110*, 16827. Schaller, R. D.; Sykora, M.; Pietryga, J. M.; Klimov, V. I. *Nano Lett.* **2006**, *6*, 424. Murphy, J. E.; Beard, M. C.; Norman, A. G.; Ahrenkiel, S. P.; Johnson, J. C.; Yu, P. R.; Micic, O. I.; Ellingson, R. J.; Nozik, A. J. *J. Am. Chem. Soc.* **2006**, *128*, 3241. Pijpers, J. J. H.; Hendry, E.; Milder, M. T. W.; Fanciulli, R.; Savolainen, J.; Herek, J. L.; Vanmaekelbergh, D.; Ruhman, S.; Mocatta, D.; Oron, D.; Aharoni, A.; Banin, U.; Bonn, M. *J. Phys. Chem. C* **2007**, *111*, 4146.
- (5) Ellingson, R. J.; Beard, M. C.; Johnson, J. C.; Yu, P. R.; Micic, O. I.; Nozik, A. J.; Shabaev, A.; Efros, A. L. *Nano Lett.* **2005**, *5*, 865.
- (6) Schaller, R. D.; Petruska, M. A.; Klimov, V. I. *Appl. Phys. Lett.* **2005**, *87*, 253102. Beard, M. C.; Knutsen, K. P.; Yu, P. R.; Luther, J. M.; Song, Q.; Metzger, W. K.; Ellingson, R. J.; Nozik, A. J. *Nano Lett.* **2007**, *7*, 2506.
- (7) Schaller, R. D.; Agranovich, V. M.; Klimov, V. I. *Nat. Phys.* **2005**, *1*, 189.
- (8) Schaller, R. D.; Pietryga, J. M.; Klimov, V. I. *Nano Lett.* **2007**, *7*, 3469.
- (9) Nair, G.; Bawendi, M. G. *Phys. Rev. B* **2007**, *76*, 081304.
- (10) Ben-Lulu, M.; Mocatta, D.; Bonn, M.; Banin, U.; Ruhman, S. *Nano Lett.* **2008**, *8*, 1207.
- (11) Antoncik, E. *Czech. J. Phys.* **1957**, *7*, 674.
- (12) Shabaev, A.; Efros, A. L.; Nozik, A. J. *Nano Lett.* **2006**, *6*, 2856.
- (13) Franceschetti, A.; An, J. M.; Zunger, A. *Nano Lett.* **2006**, *6*, 2191.
- (14) Allan, G.; Delerue, C. *Phys. Rev. B* **2006**, *73*, 205423. Allan, G.; Delerue, C. *Phys. Rev. B* **2008**, *77*, 125340.
- (15) Henry, C. H.; Lang, D. V. *IEEE Trans. Electron Devices* **1974**, *21*, 745. Englman, R.; Jortner, J. *Mol. Phys.* **1970**, *18*, 145.
- (16) Woggon, U.; Giessen, H.; Gindele, F.; Wind, O.; Fluegel, B.; Peyghambarian, N. *Phys. Rev. B* **1996**, *54*, 17681. Klimov, V. I.; McBranch, D. W. *Phys. Rev. Lett.* **1998**, *80*, 4028. Wehrenberg, B. L.; Wang, C.; Guyot-Sionnest, P. *J. Phys. Chem. B* **2002**, *106*, 10634. Schaller, R. D.; Pietryga, J. M.; Goupalov, S. V.; Petruska, M. A.; Ivanov, S. A.; Klimov, V. I. *Phys. Rev. Lett.* **2005**, *95*, 196401.
- (17) Isborn, C.; Kilina, S.; Li, X.; Prezhdo, O. V. Submitted for publication.
- (18) Rabani, E.; Hetenyi, B.; Berne, B. J.; Brus, L. E. *J. Chem. Phys.* **1999**, *110*, 5355.
- (19) Williamson, A. J.; Zunger, A. *Phys. Rev. B* **2000**, *61*, 1978.
- (20) Kim, J. N.; Wang, L. W.; Zunger, A. *Phys. Rev. B* **1998**, *57*, R9408.
- (21) Toledo, S.; Rabani, E. *J. Comput. Phys.* **2002**, *180*, 256. Wall, M. R.; Neuhauser, D. *J. Chem. Phys.* **1995**, *102*, 8011.
- (22) Baer, R.; Seideman, T.; Ilani, S.; Neuhauser, D. *J. Chem. Phys.* **2004**, *120*, 3387.
- (23) Wang, L. W.; Zunger, A. *Phys. Rev. B* **1996**, *53*, 9579.
- (24) Hendry, E.; Koeberg, M.; Wang, F.; Zhang, H.; Donega, C. d. M.; Vanmaekelbergh, D.; Bonn, M. *Phys. Rev. Lett.* **2006**, *96*, 057408.

NL802443C